International Journal of Thermophysics, Vol. 28, No. 2, April 2007 (© 2007)
DOI: 10.1007/s10765-007-0171-5

Surface Position-Resolved Thermophysical Properties for Metallic Alloys

Y. W. Kim[1,2]

Thermophysical properties are collective measures of a material to transport dynamical quantities of physical nature on its surface or through the bulk. As such, the exact nature of couplings between particles in a many-body assembly of building block atoms or molecules sensitively determines their values. The couplings between nearest neighbors are the product of the local elemental composition and the material phase. In this study, thermal cycling of a four-element Wood's alloy specimen brings out cadmium-rich patches to the top surface of the specimen. An assembly of such patches leads to depth-dependent deviations of elemental composition from that of the bulk. Surface-layer atoms are driven to form a high temperature laser-produced plasma (LPP), and time-resolved spectroscopy of their emissions show the variability of elemental composition over surface positions as well as over depth from the surface. These thermal history-driven composition anomalies contribute to significant variability in the measured values of spectral emissivity and thermal diffusivity.

KEY WORDS: Benard–Marangoni instability; near-surface composition anomaly; position-resolved composition; Wood's alloy.

1. INTRODUCTION

One of the factors that affects thermophysical property determination is compositional and morphological property nonuniformity in a material specimen. This has been made self evident in simultaneous measurements of the composition and thermal diffusivity by using the method of time-resolved spectroscopy of laser-produced plasma (LPP) plume emissions

[1] Department of Physics, Lewis Laboratory 16, Lehigh University, Bethlehem, Pennsylvania 18015, U.S.A.
[2] To whom correspondence should be addressed. E-mail: ywk0@lehigh.edu

from the specimen surface for a number of alloy specimens [1]. A submicron layer is removed from each laser excitation [2]. Repetitive LPP measurements applied to a specimen exhibit systematic drift in the measured values of spectral emissivity and thermal diffusivity as the material composition undergoes changes. The trend continues with increasing depth, although diminishing with depth. We have pinpointed that the variability is traceable to the depth dependence of the near-surface elemental composition in each of the specimens studied [2, 3].

Of interest is whether the reasons for the development of such depth-dependent composition are intrinsic to the metallic alloy systems. Our studies with the model system of Wood's alloy have shown that it is possible to drive the elemental composition of a surface layer away from the composition of the bulk by thermal cycling of a specimen between heating to 393°C and resolidification [4]. It is quite possible to speculate that the depth dependence is manifest due to a distribution of patches of segregated elements at the surface, whose feature size and shape are irregular and depth dependent due to thermo-fluid dynamic instability during melting and solidification. In previous studies [2–4], composition variations were examined as a function of depth; element specific emission intensities were integrated over the focal area of the laser beam that excites the material surface. The focal area is oblong in shape, 2.3 mm long and 1.3 mm wide. In this article, we examine, across the focal area on the surface, the position-dependent variation of the specimen's elemental composition on, and near, the surface of the Wood's alloy specimens. The surface position dependence is determined over the focal area on the specimen's surface, and the depth dependence is analyzed by successive LPP excitation.

We present a description of the experimental setup and the procedure by which the measurement has been carried out. The steps by which the near-surface composition evolves during thermal cycling are examined.

2. EXPERIMENTAL ARRANGEMENT

The specimen of interest is placed on a heater stage inside a small vacuum chamber. A Q-switched laser pulse is directed at the specimen directly from above through a focusing lens that is an integral part of the vacuum chamber [2–4]. The experimental setup has two additional capabilities implemented: (a) one-to-one spectroscopic imaging of the laser focal area of the specimen's surface onto the entrance slit of a spectrograph and (b) a capability to translate the specimen stage within the vacuum chamber by an x-y translation stage that is positioned outside the vacuum chamber. The objective here is to associate the plasma emission spectra with points on the specimen's surface along an axis that runs along

the center of the entrance slit. For each such point, full spectral information is detected, from which the elemental composition of the material at that location can be determined.

Translation of the specimen can be achieved to one-micron resolution over a 3 mm by 3 mm area. We have, however, concluded that this resolution is difficult to realize from the standpoint of spectroscopy because to limit the focal area of the laser pulse to the minimum area of resolution is not practical; besides, there is a non-trivial chance that nanoparticles resulting from one LPP plume can settle on the adjacent area from the focal spot [5]. The translation capability is thus used only to explore the surface areas of interest on a given specimen.

Figure 1 shows the experimental arrangement schematically. The heating stage is machined out of a solid copper cylinder. The top end has a recess in the form of a cylindrical indentation, 18.0 mm in diameter and 5.1 mm in depth. Heating of the block is done by electrical heating of a Nichrome ribbon, 4.8 mm wide and 0.2 mm thick, that runs through a diametrical hole at the bottom of the block; the ribbon also supports the block. A blind hole is drilled in the block, and an alumel-chromel thermocouple is inserted for measurement of the temperature of the block.

A specimen is prepared by melting irregularly shaped rods of Wood's alloy in a small crucible, which is placed inside the cylindrical recess at the top of the heating block. The crucible is made of aluminum or boron nitride; the latter was effective because it is non-wetting to Wood's alloy. The crucible has outside dimensions of 17.8 mm in diameter and 5.1 mm in thickness. The crucible's interior volume has the shape of a thin disk with a diameter of 16.3 mm or 17.5 mm, depending on whether an additional lining of boron nitride was used. The thickness of the molten specimen varied from 0.4 to 3.8 mm.

3. SPECIMEN PREPARATION

The batch of Wood's alloy used in this study has the manufacturer's composition as follows: 50 mass% bismuth, 25 mass% lead, 12.5 mass% tin, and 12.5 mass% cadmium. A sample is loaded into the crucible by melting the tip of a rod of Wood's alloy while the crucible is heated to $135 \pm 10°C$ in the heating stage. It is cooled to a solid disk in an open atmosphere. The vacuum chamber is evacuated to 1.3×10^2 Pa and filled with argon to 10^5 Pa; this is to localize the re-solidifying vapors of Wood's alloy during the thermal cycling period in the immediate vicinity of the heating stage.

The specimen is heated at an approximately constant heating rate to 393°C over a time period of 13–15 min. This temperature is above what

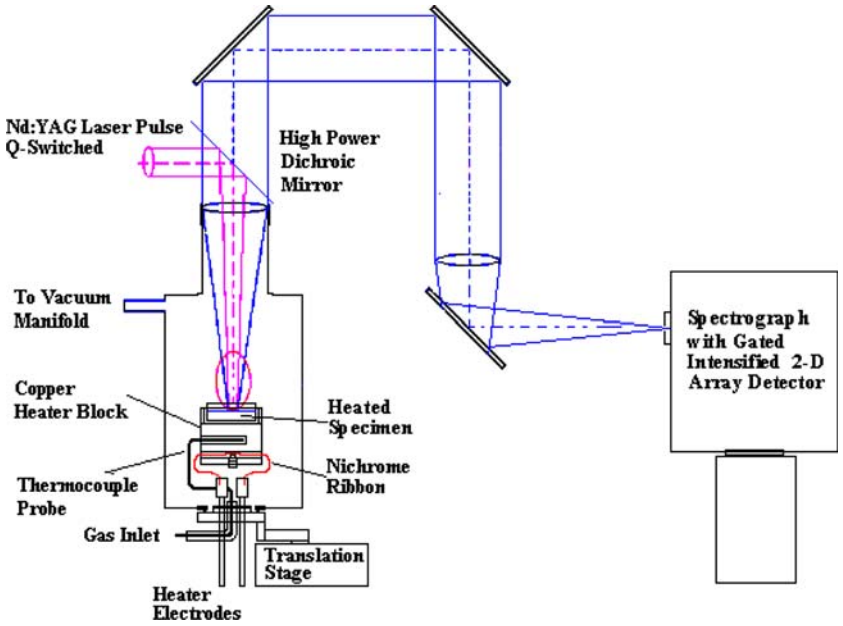

Fig. 1. Key components of the experimental setup are shown schematically: the vertical dome of the vacuum chamber, housing a specimen heating block; a translatable platform; the 3-D optics for both projecting a high-power laser pulse onto the specimen and forming an image of the footprint of an LPP plume on the entrance slit plane of a spectrograph; and a gated intensified array detector mounted on the image plane of the spectrograph. The Q-switched Nd:YAG laser, vacuum pumps, gas supply handling manifold, and digital timing and recording electronics are not shown.

appears to be a threshold temperature for a significant modification of Wood's alloy composition at the surface [2–4]. The full round of heating may be repeated up to three times with each specimen in order to accentuate the elemental composition anomaly. The general appearance of the specimen's surface is a gradual darkening from light metallic gray to patchy black for each successive heating cycle. The cross section of the specimens used for this round of study is larger by up to a factor of four, and the darkening is manifest by emergence of black patches that grow larger and more numerous with the increased number of heating cycles. The process seems best characterized by a Benard–Marangoni instability; the evidence is described in a separate accompanying article [6].

4. POSITION-RESOLVED COMPOSITION ANALYSIS

The appearance of darkened patches on the surface of the thermally cycled specimen of Wood's alloy is the leading indicator of movement in

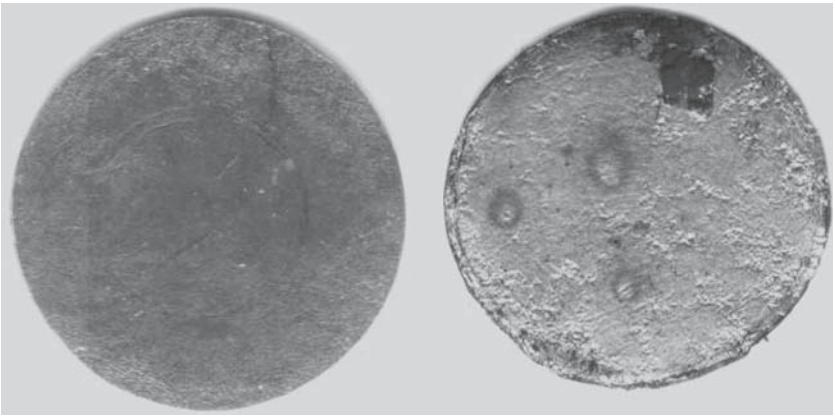

Fig. 2. Scanned images of a 0.8-mm thick specimen of Wood's alloy are shown: (a) before thermal cycling and (b) after one round of 13-min thermal cycling with the top of the specimen crucible open to the atmosphere of argon at one atm. Darkened patches appear on the specimen's surface.

the elemental composition profile in space. These patches appear only if heating is applied nonuniformly over the specimen, and repetitive application of the heating cycle broadens the islands and increases the number density of islands [6]. Figure 2 shows a sample image of a Wood's alloy specimen (a) before the specimen is treated in a heating cycle; and (b) after one round of heating to 393°C. A few patches are visible, but they appear irregularly distributed on the surface. In this article we report on position-resolved analysis of a patch for elemental composition.

The first approach we considered was to carry out point-to-point analyses over an area on the surface. This was abandoned for two reasons: one, it takes too long to cover a selected surface area with sufficient position resolution; and two, a LPP plume from an analysis event contaminates the adjacent points in the form of nano-particle deposits due to condensation of the matter in the plume [5]. We have instead achieved position-resolved analysis by position resolving the structure of plasma emissions within the surface footprint of an LPP plume.

A top view of the footprint of the plume is focused on the plane that contains the entrance slit of a spectrograph with unity magnification. This gives a one-dimensional (1-D) section of the footprint of the LPP plume from the specimen's surface with a 10-μm-scale resolution along the axis collinear with the entrance slit. The exit plane of the spectrograph is equipped with a 2-D array detector so that the spectra of the plume's emissions from individual surface points are resolved along the direction

of the entrance slit height. A 256 detector pixels are allocated over the 6.2-mm position span; 1024 pixels are available for each surface point to capture emissions over the selected spectral range. The ultimate position and spectral resolutions are determined by the image magnification and the spectral dispersion of the spectrograph, respectively. The spectral dispersion used in this study is 0.17 nm per pixel.

The intensity distribution across the focal spot of the laser pulse is not uniform; it is approximately Gaussian with some non-negligible distortions. This means that the excitation of the surface elements into various internal upper-level states of the respective atoms and ions must be calibrated at each pixel point of the surface along the axis of the entrance slit of the spectrograph. In other words, each of more than a quarter of a million pixels must be calibrated for the response of 256 surface points to laser excitation at varying incident laser intensities. The procedure that we have found effective involves normalization of the pixel responses to LPP plume emissions from a thermally cycled specimen to the responses from the same specimen before any thermal cycling. The laser power density and placement of the image of the focal spot of the pulsed laser on the entrance slit of the spectrograph are held fixed for the two separate LPP excitations for the calibration.

Figure 3a shows the two sets of respective emission spectra, one from a single thermal cycling of the specimen (b) and another from the fresh specimen (a). Figure 3b displays the pixel-by-pixel intensity ratio of the two spectra as a function of position along a line cutting across the patch. Here, if there had been no change in the emission intensity (i.e., no change in elemental composition at the selected surface point), the ratio would remain at unity, leaving the corresponding percentage change at zero.

The above discussion leads to the specific pathway along which changes in elemental composition are evaluated at each of the surface points that have been selected by the entrance slit of the spectrograph. The following emission lines are used to track the abundance of bismuth, lead, tin, and cadmium: 472.952 nm BiI and 473.03 nm BiII; 405.7807 nm PbI; 452.474 nm SnI; and 479.9912 nm CdI. The product of the atomic transition probability and the population of radiating atoms or ions within the LPP plume determine the intensity of each emission line [7], and therefore each spectral line-intensity must be converted into mass% by multiplying with a constant. The full set of the constants at each surface point is determined by the reference spectrum. The surface position-resolved composition for the thermally cycled specimen is determined according to the set of scaling constants, or equivalently, from the percent deviation of the line emission intensities from those of the reference specimen. These sets of constants are surface position-dependent because the incident intensity

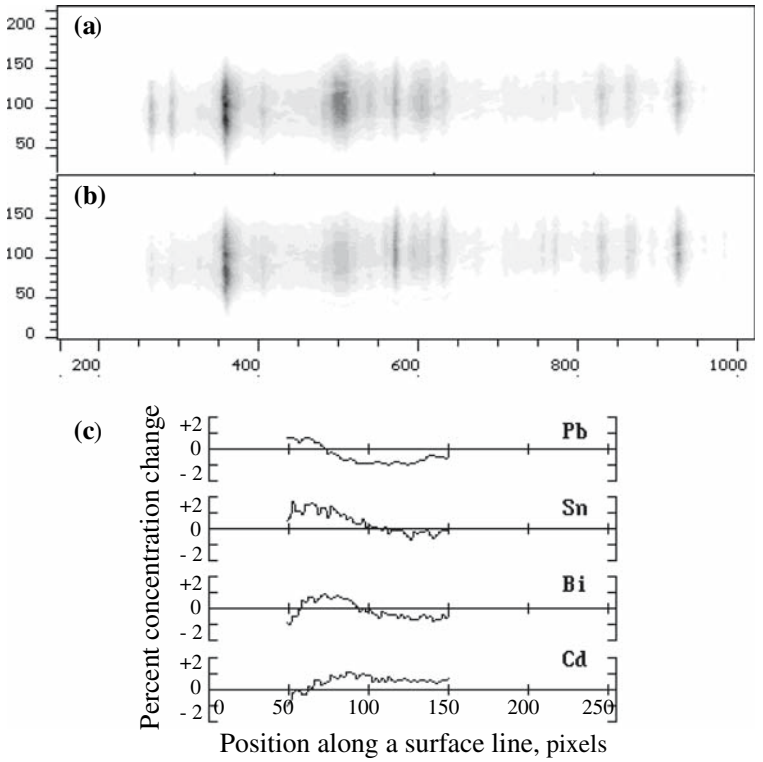

Fig. 3. (a) Emission spectra from an LPP plume from a darkened patch that appears on the specimen's surface after one round of thermal cycling, (b) emission spectra from another LPP plume from a fresh Wood's alloy specimen as a calibration reference, and (c) percent changes in individual elemental concentrations as functions of position along a line that cuts across one of the darkened patches that appear on the surface of the thermally cycled specimen. Adjacent detector pixels are separated by 24.8 μm along the line that cuts across the darkened patch on the specimen's surface.

of the laser pulse varies as a function of the surface position. Use of the reference specimen conveniently attends to all such aspects of the calibration process.

The position-resolved elemental composition as deduced from the intensity data in Fig. 3 is shown in Fig. 4. Movements of the elemental concentrations can be seen as one crosses the outer perimeter of the LPP-ablated patch in question.

An absolute determination of measurement errors is difficult to carry out because there is no longer a reliable objective standard for elemental

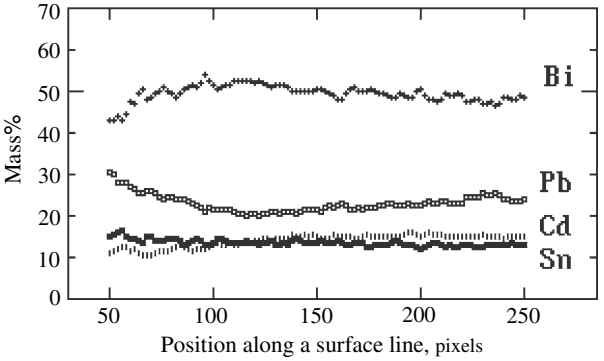

Fig. 4. Measured composition (mass%) as a function of position along a line that cuts across a darkened patch on the surface of a once-heated Wood's alloy specimen. Position dependence is obtained from quantitative analysis of the data shown in Fig. 3c. The four constituent elements of the specimen are seen to show significantly modified compositions as functions of position along the line through the patch: bismuth (crosses), lead (squares), cadmium (lines), and tin (filled squares).

composition for this study. We can, however, make an estimate for the range of uncertainties in determining the emission line intensities on the basis of counting rate uncertainties. Here, the photon-counting rate has ranged from about 4500 to 14800 detected photoelectrons at each detector pixel during the integration time of 400 ns. This would set the maximal uncertainty in the photoelectron-counting rate at 1.50% to 0.82%. In making a comparison of the elemental abundances in the thermally cycled specimen to those in the fresh reference specimen, the reproducibility of the total laser pulse energy matters; we have controlled the laser operation to keep it less than 2.00% from one shot to another. (The mode amplitudes within a laser pulse may still vary relative to each other from one shot to the next, but we do not have any estimates for how the intensity profile changes within a laser pulse). Together, these will hold the uncertainty in elemental concentrations due to thermal cycling to within 3%.

5. CONCLUDING REMARKS

In this study, we have gained more knowledge about how the surface elemental composition becomes driven away from the bulk composition—namely, the near-surface composition anomaly is brought about

by accumulation of cadmium-rich patches on the surface, which grow in size and number with increasing rounds of thermal cycling. A companion study [6] further examines the possible role of convection accompanying thermal cycling of a specimen of Wood's alloy. Earlier studies discovered substantial modifications of the elemental composition of the near-surface layers of the alloy if the mean bath temperature exceeds a threshold value [2, 3]. Studies of the dynamics of a slab of fluid under heating from below predict convection rolls or cells if a critical temperature gradient within the bath is realized. Our experimental arrangement has that the top surface of the specimen is open, thus radiating freely into the vacuum chamber space while the bottom surface is constrained by the base surface of the crucible. It is therefore likely that the specimen experiences a vertical temperature gradient. Given the disparate melting points of the constituent elements within the alloy, it is most likely that thermophysical properties, particularly the surface tension, of the multi-element alloy develop position dependence along with changing temperature. It behooves us to consider the possible role of Benard–Marangoni instability [8, 9] in the near-surface composition anomaly. Observation suggests the existence of a thin membrane-like solid layer at the surface is quite plausible, and if true, it will in turn drive separations of elements due to the different elemental melting points. The mystery is in the absence of any discernable regularity in the distribution of the surface patches [6], unlike those convection patterns commonly seen in the studies of the instability with transparent liquids [10–12].

We further note that the elemental composition profile differs from one patch to another, but whether this is due to differences in the intrinsic composition structure within each patch or caused by the discreteness of the LPP ablation depth remains undetermined at present.

REFERENCES

1. Y. W. Kim, *Int. J. Thermophys.* **14**:397 (1993).
2. Y. W. Kim, *Int. J. Thermophys.* **25**:575 (2004).
3. Y. W. Kim, in *Thermal Conductivity*, Vol. 26, R.B. Dinwiddie, ed. (DES*tec* Pubs., Lancaster, Pennsylvania, 2005), pp. 146–158.
4. Y. W. Kim, *Int. J. Thermophys.* **26**:1051 (2005).
5. Y. W. Kim, H.-D. Lee, and P. Belony, Jr., *Rev. Sci. Instrum.* (in press).
6. Y. W. Kim, *Int. J. Thermophys.* (in press).
7. Y. W. Kim, in *Laser-Induced Plasmas and Applications*, L. J. Radziemski and D. A. Cremers, eds. (Marcell Dekker, New York, 1989), Chap. 8.
8. P. Kundu, *Fluid Mechanics* (Academic Press, New York, 1990).
9. M. I. Char, and K. T. Chiang, *J. Phys. D: Appl. Phys.* **27**:748 (1994).

10. T. Ondarcuhu, G. Mindlin, H. Mancini, and C. Perez-Garcia, *Phys. Rev. Lett.* **70**:3892 (1993).
11. T. Ondarcuhu, G. Mindlin, H. Mancini, and C. Perez-Garcia, *J. Phys.: Condens. Matter* **6**:A427 (1994).
12. S. Hoyas, A. M. Mancho, H. Herero, N. Garnier, and A. Chiffaudel, *Phys. Fluids* **17**:054104 (2005).